ELSEVIER

Biophysical Chemistry 50 (1994) 129–138

Biophysical Chemistry

Intracellular signaling through long-range linked functions in the Ca^{2+} transport ATPase

Giuseppe Inesi, Ziyu Zhang, Yutaka Sagara, Mary E. Kirtley

Department of Biological Chemistry, School of Medicine, University of Maryland, Baltimore, MD 21201, USA

(Received 5 January 1994)

Abstract

The Ca^{2+} transport ATPases of intracellular membranes exhibit an intracellular long-range functional linkage which is the basic mechanistic device for Ca^{2+} transport through ATP utilization. The functional linkage operates between a phosphorylation (catalytic) domain located in the extramembranous region, and a Ca^{2+} binding domain located in the membrane bound region of the enzyme. The two domains are separated by a distance of ≈ 50 Å, and are both affected by binding of a single molecule of the highly specific inhibitor, thapsigargin, to the enzyme. Functional and structural features are here described to explain the long-range linkage through the protein structure.

Key words: Intramolecular signaling; Ca^{2+} transport; SERCA ATPases; Thapsigargin; Ca^{2+} binding domain; Linked functions

1. Introduction

The sarco- and endo-plasmic reticulum Ca^{2+} (SERCA) ATPases constitute a family of homologous enzymes that are involved in active transport of Ca^{2+} into intracellular stores [1–5], thereby regulating the concentration of cytosolic Ca^{2+}. The SERCA ATPases share the common feature of being specifically inhibited by thapsigargin, a plant-derived sesquiterpene lactone. A most interesting characteristic of these enzymes is the allosteric mechanism of catalytic and transport coupling, and of inhibition by thapsigargin. Elements of function and topology are here described, providing evidence of a long-range linkage of functional domains within the ATPase molecule. The information derives mostly from studies of the sarcoplasmic reticulum ATPase, the first of these enzymes to be discovered and characterized [6,7].

2. Functional linkage of Ca^{2+} binding and phosphoenzyme formation

The basic mechanistic feature of the Ca^{2+} ATPase catalytic and transport cycle can be demonstrated by presteady state experiments showing that formation of a phosphorylated enzyme intermediate and simultaneous internalization (or occlusion) of two moles of bound calcium per mole of enzyme occurs following addition of

SSDI 0301-4622(94)00014-B

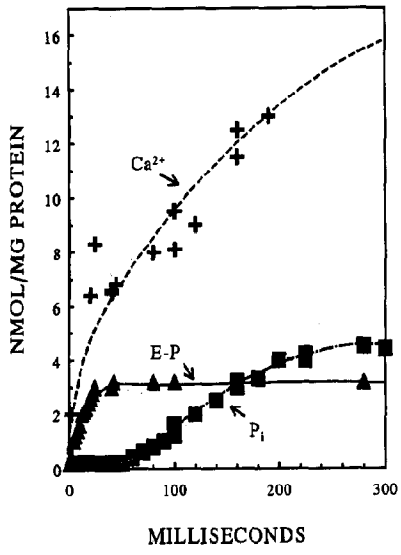

Fig. 1. Formation of phosphorylated enzyme intermediate (EP), internalization of bound Ca^{2+}, and hydrolytic P_i cleavage, following addition of ATP to sarcoplasmic reticulum vesicles preincubated with Ca^{2+}. Time resolution was obtained with rapid quench methods [8].

ATP to enzyme preincubated with Ca^{2+} (Fig. 1). Hydrolytic cleavage of the phosphoenzyme follows after a lag period, thereby permitting repeat cycles and the onset of steady state activity. The same kinetic sequence is obtained when ATP is replaced by acetylphosphate and other phosphorylated substrates, indicating that the adenosine moiety of the substrate is not essential to the transduction mechanism. It is, rather, the phosphorylation reaction that plays an essential role in causing vectorial displacement of bound Ca^{2+} from the enzyme. This can be understood in quantitative terms from the following sequence of partial reactions and their equilibrium constants, which were characterized in the presence of saturating Mg^{2+}, neutral pH and 25°C [9]:

$$H_2E + 2Ca^{2+}_{out} \rightleftharpoons E \cdot Ca_2 + 2H^+_{out} \quad (3 \times 10^2\ M^{-2}), \tag{1}$$

$$E \cdot Ca_2 + ATP \rightleftharpoons ATP \cdot E \cdot Ca_2 \quad (1 \times 10^5\ M^2), \tag{2}$$

$$ATP \cdot E \cdot Ca_2 \rightleftharpoons ADP \cdot E\text{–}P \cdot Ca_2 \quad (0.3), \tag{3}$$

$$ADP \cdot E\text{–}P \cdot Ca_2 \rightleftharpoons E\text{–}P \cdot Ca_2 + ADP \quad (7 \times 10^{-4}\ M), \tag{4}$$

$$E\text{–}P \cdot Ca_2 + 2H^+_{in} \rightleftharpoons H_2E\text{–}P + 2Ca^{2+}_{in} \quad (3 \times 10^{-6}\ M^2), \tag{5}$$

$$H_2E\text{–}P \rightleftharpoons H_2E \cdot P_i \quad (1), \tag{6}$$

$$H_2E \cdot P_i \rightleftharpoons H_2E + P_i \quad (1 \times 10^{-2}\ M), \tag{7}$$

The cycle begins with high affinity acquisition (reaction (1)) of Ca^{2+} from the outer medium, in exchange for H^+. Ca^{2+} binding is required for activation of the enzyme, thereby permitting utilization of ATP and formation of a phosphorylated intermediate (reactions (2)–(4)). In turn, enzyme phosphorylation destabilizes and changes the vectorial orientation of the bound Ca^{2+}, increasing the probability of its dissociation into the lumen of the vesicles in exchange for lumenal H^+ (reaction (5)). Note that the equilibrium constant for the enzyme phosphorylation by ATP is nearly 1, indicating that the free energy of ATP is conserved by the enzyme, and utilized to change the Ca^{2+} binding characteristics. Finally, the phosphoenzyme undergoes hydrolytic cleavage and releases P_i (reactions (6) and (7)) before entering another cycle. The reaction sequence then shows clearly that the *direct mechanistic device for cation translocation against a gradient is enzyme phosphorylation, rather than hydrolytic cleavage of P_i* [10].

As the catalytic and transport cycle is likely to include isomeric transitions in addition to the chemical reactions listed above, it should be noted that such transitions are coupled implicitly with the chemical reactions subjected to experimental measurement, and their influence is reflected by the equilibrium constants given above. In fact, the standard free energies ($-RT \ln K$) of the partial reactions add up to the standard free energy of ATP hydrolysis (γ-phosphate), as expected. Most interestingly, the standard free energy diagram for the partial reactions reveals that the chemical potential of ATP does not manifest itself in the phosphoryl transfer or hydrolytic cleavage reactions (K_4 and K_6 near 1), but rather

in the drastic reduction of the enzyme affinity for Ca^{2+} (compare K_1 to $1/K_5$). We can then write that, under standard conditions

$$\Delta G = RT \ln\left(K_a^{CaEP}/K_a^{CaE}\right),$$

per n number of calcium ions transported per cycle. K_a^{CaE} and K_a^{CaEP} are the *association* constants of the enzyme for Ca^{2+} in the ground state and following activation by ATP, respectively. With reference to the reaction scheme given above, the two relevant constants are K_1 and $1/K_5$. Correction of the standard free energy diagram for the actual concentrations of substrates and products (i.e. ATP, ADP, P_i, Ca^{2+}_{out}, Ca^{2+}_{in}) yields net free energy changes which determine the forward or reverse direction of net fluxes [8,11,12].

3. Inhibition by thapsigargin

Thapsigargin is a sesquiterpene lactone isolated from root extracts of Thapsia garganica [13] which was found to inhibit the endoplasmic [14] and sarcoplasmic [15] reticulum Ca^{2+} pumps. It was then established that thapsigargin is a highly specific inhibitor of all tested intracellular Ca^{2+} transport ATPases [5,16,17]. The inhibitory effect is produced by amounts of thapsigargin stoichiometrically equivalent to the ATPase present in the reaction mixture, with a dissociation constant lower than nanomolar. The inhibition affects Ca^{2+} transport as well as Ca^{2+} dependent ATPase activity.

Studies of the mechanism of inhibition by thapsigargin reveals that both the Ca^{2+} binding and phosphorylation functions are affected by interaction of the enzyme with one mol of thapsigargin. Ca^{2+} binding (reaction (1) in the sequence given above) measured under equilibrium conditions in the absence of ATP, is found to be inhibited by thapsigargin. On the other hand, enzyme phosphorylation with P_i (reverse of reactions (6) and (7) in the sequence given above) measured under equilibrium conditions in the absence of Ca^{2+}, is also found to be inhibited by thapsigargin [18]. These experiments demonstrate that two partial reactions occurring in distant domains within the enzyme molecule, are inhibited by thapsigargin under conditions permitting their occurrence independent of each other (i.e. not requiring enzyme cycling). It is then apparent that thapsigargin is a global inhibitor inasmuch as its effect is transmitted over a long distance through the enzyme structure [19]. In fact, this long-range effect determines, under appropriate conditions, whether the ATPase does or does not form bidimensional crystalline arrays within the plane of the membrane [20].

4. Topology of the Ca^{2+} ATPase

The Ca^{2+} ATPase is a membrane spanning protein composed of a single polypeptide chain of 1001 amino acids. A variety of physical methods, including electron microscopy and diffraction patterns [21–26], have revealed that the enzyme has a pear-shaped structure with a large lobe projecting from the cytosolic side of the mem-

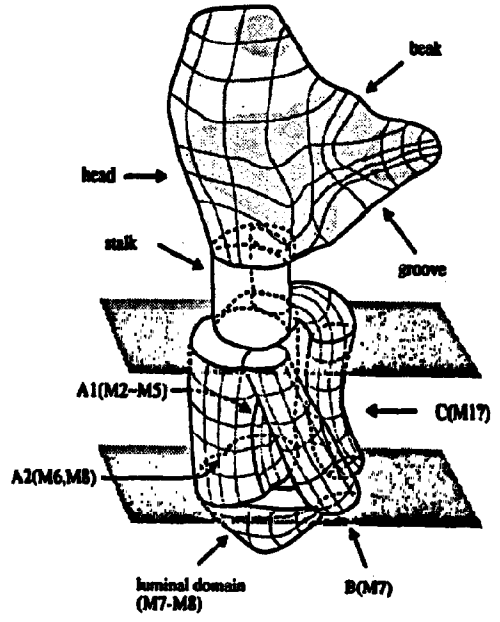

Fig. 2. Three-dimensional image of the sarcoplasmic reticulum ATPase obtained by cryo-electron microscopy. The extramembranous cytosolic region of the enzyme is shaped as a head with a beak, connected through a stalk to ten membrane spanning helices [27].

brane and only a much smaller mass emerging from the lumenal side of the membrane (Fig. 2). The amino acid sequence was determined by a combination of direct protein sequencing [28] and cDNA sequencing [1,29]. The hydropathy plot reveals ten hydrophobic regions which are likely to be transmembrane helices. Both the N-terminal and C-terminal residues are located on the cytosolic side of the membrane.

If we consider the distribution of the ATPase sequence with respect to the membrane (Fig. 3), we find that the residue undergoing phosphorylation (Asp351) resides within the large extramembranous loop. Furthermore, covalent modification of residues in the large extramembranous loop (for review see Bigelow and Inesi [30]) interfere with ATP binding. Therefore the entire *catalytic and phosphorylation domain* is located within this loop which corresponds to the large cytosolic lobe in the folded structure of the protein (Fig. 2).

Location of the *two* Ca^{2+} *binding sites* has been greatly assisted by site-specific mutagenesis. It was demonstrated [31] that replacement of any one of the residues Glu 309, Glu 771, Asn 796, Thr 799, Asp 800, Glu 908 results in inactivation of the pump. Each of these mutant proteins can be phosphorylated at the active site by reversal of

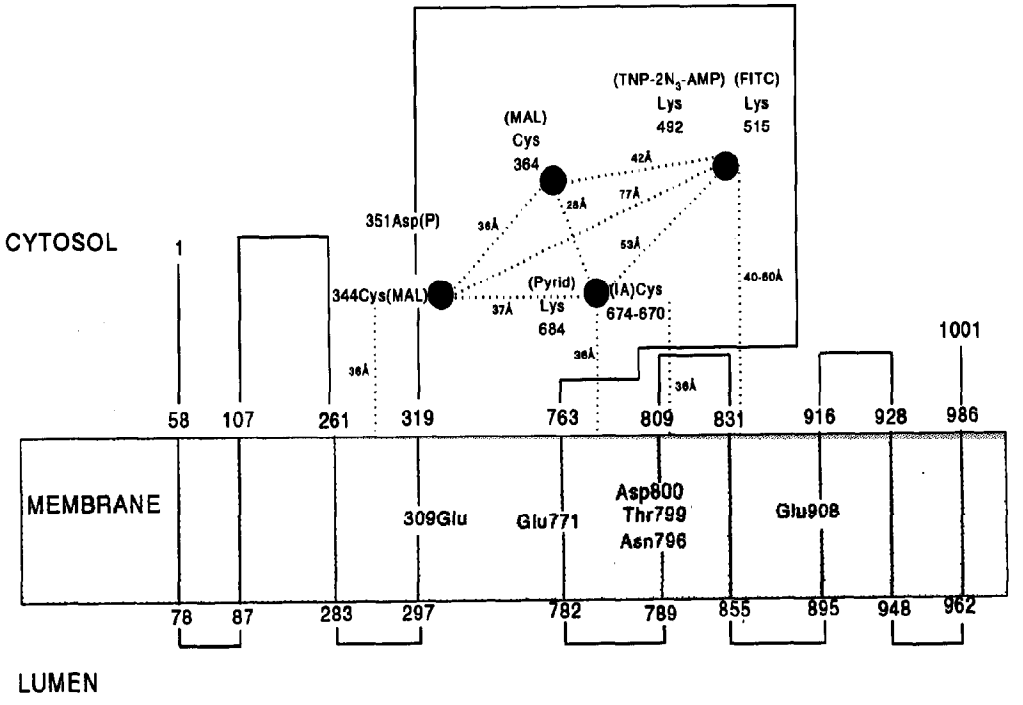

Fig. 3. Topology of the Ca^{2+}-ATPase in the sarcoplasmic reticulum membrane. The diagram shown is based on the analysis of MacLennan et al. and Clarke et al. [1,31], and derivatization of various residues as reviewed by Bigelow and Inesi [30]. The cytosolic head structure is composed of two major segments. The larger, residues 319 to 763, contains the catalytic site Asp351, which is phosphorylated during catalytic turnover, and the ATP binding site. The smaller cytosolic loop, residues 107 to 261, is likely to participate in the folded structure of the larger loop. The transmembrane segments include residues Glu309, Glu771, Asp800, Thr799, Asn796, and Glu908, involved in Ca^{2+} binding functions. Specific points of reference are shown in the extramembranous region, including cysteine residues that are reactive to fluorescent maleimide (MAL) or iodoacetamide (IA) derivatives, as well as the site of FITC derivatization. The points of reference corresponding to the related chromophores are shown as black dots, in a trigonal arrangement as suggested by spectroscopic studies. Lys492 (derivatized by TNP-N_3-AMP), Lys684 (derivatized by ATPpyridoxal), and Asp351 (undergoing phosphorylation upon utilization of ATP) are shown near the appropriate points of references.

the normal reaction, i.e. by phosphorylation with P_i. Ordinarily this reaction is totally blocked in the presence of Ca^{2+}. However, in the mutant proteins Ca^{2+} fails to block phosphorylation from P_i. Thus all of these residues are required for Ca^{2+} linked functions. Inspection of Fig. 3 reveals that all six residues linked to Ca^{2+} functions are located in the transmembrane section of the protein, as also indicated by direct measurements of Ca^{2+} binding and its inhibition by carbodiimide labels partitioned in the membrane [32,33].

Further evidence for location of the Ca^{2+} binding domain within the membrane bound region of the ATPase is provided by the functional behavior of two chimeric proteins [34] in which large extramembranous segments including the catalytic domain are derived from the Na^+, K^+ ATPase alpha subunit, while the flanking segments derive from the skeletal (SERCA 1) or cardiac (SERCA 2) SR Ca^{2+} ATPase. The chimeric proteins are obtained by transfection of recombinant DNA in mammalian cells, and the expressed proteins are recovered in the microsomal fraction of the transfected cells. Functional studies indicate that these chimeras exhibit very slow turnover and very poor Ca^{2+} transport activity, when compared with wild-type enzyme. Nevertheless, the chimeric proteins are able to form normal levels of phosphorylated intermediate by utilization of radioactive ATP. Most importantly: (1) formation of the intermediate is strictly Ca^{2+} dependent; and (2) formation of the intermediate is inhibited by thapsigargin. Therefore, the chimeric proteins retain Ca^{2+} dependence and inhibitor sensitivity, just as the original Ca^{2+} ATPase, even though ATP binding and phosphorylation of the Asp351 occurs on the half of the molecule derived from a Na^+K^+ ATPase. This indicates that the Ca^{2+} binding domain (specific for the Ca^{2+} ATPase) cannot reside within the cytoplasmic domain (derived from the Na^+, K^+ ATPase), and is consistent with its location within the membrane bound region.

5. Distances between sites on the Ca^{2+}ATPase

Derivatization of specific residues has contributed significantly to our understanding of the Ca^{2+} ATPase, as reviewed by Bigelow and Inesi [30]. For example, derivatization of Lys515 [35] with FITC (fluorescein isothiocyanate) interferes with ATP binding and provides a point of reference for the nucleotide binding domain. The fluorescent properties of the FITC label can be utilized in spectroscopic studies of protein structure. It is also known that maleimide directed probes react with cysteines 344 and 364 [36,37] near the phosphorylation site (Asp351). Furthermore, iodoacetamide directed probes react with

Table 1
Molecular dimensions of the Ca^{2+}-ATPase from fluorescence energy transfer [a]

Donor	Labeled residues	Acceptor	Labeled residues	R_0	Distance (Å)
IAEDANS	Cys670, 674	FITC	Lys515	49	53
		DABmal	Cys344, 364	49	28, 37
		Pr^{3+}	not determined	9	16–18
ANSmal	Cys344, 364	FITC	Lys515	42	42, 77
		IAF	Cys670, 674	41	32, 47
		Pr^{3+}	not determined	9	14–19
		DABmal	Cys344,364	40	36
FITC	Lys515	rhodamine-PE	bilayer surface	55	> 60
tryptophans	50, 77, 107, 272, 288	IAEDANS	Cys670, 674	23	36
	552, 794, 832, 854,	DABmal	Cys344, 364	28	42
	855, 932, 928, 967	ANSmal	Cys344, 364	29	36

[a] The details and references are reviewed by Bigelow and Inesi [30].

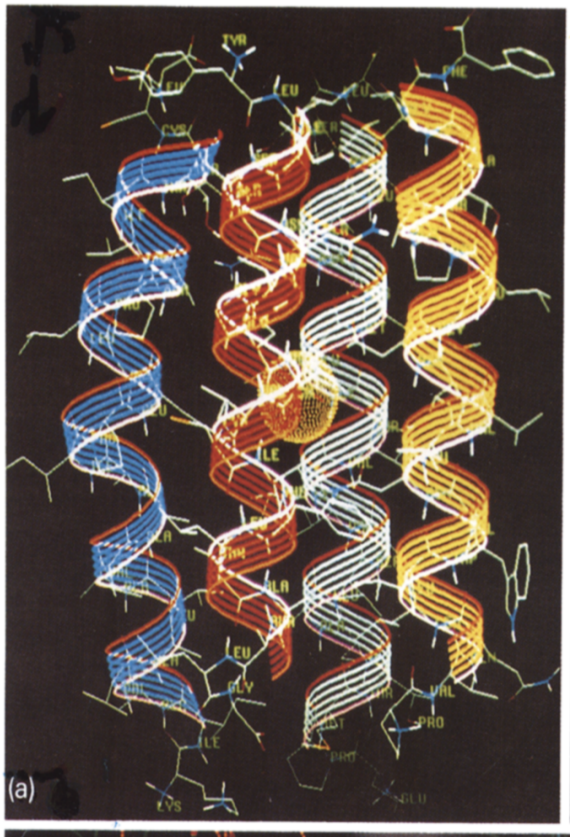
(a)

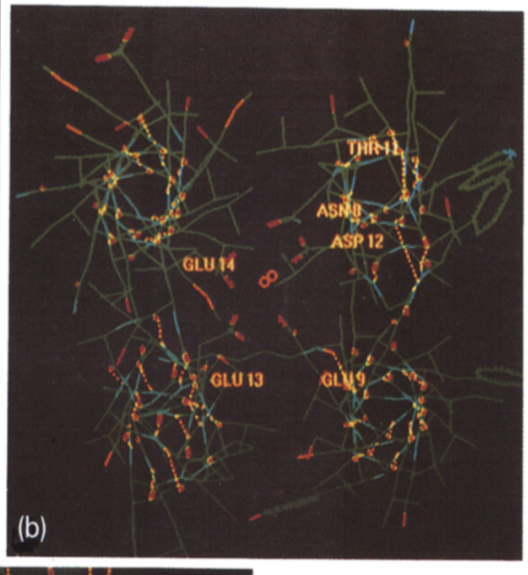
THR 11
ASN 8
ASP 12
GLU 14
GLU 13
GLU 9
(b)

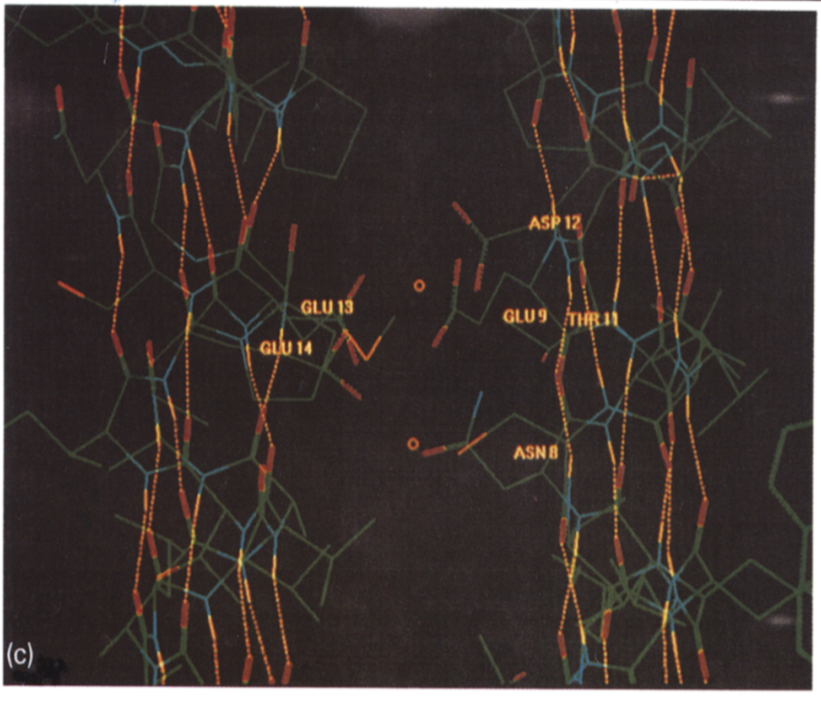
ASP 12
GLU 13
GLU 9
THR 11
GLU 14
ASN 8
(c)

cysteines 670 and 674 near the ATP binding site [38], and azido-TNP nucleotide derivatives, analogs of ATP, react with Lys 492 [39]. Some of the reactive residues have been used for fluorescence energy transfer measurements, and have yielded estimates of the distances between specific points of reference within the protein structure (Table 1 and Fig. 3). Specifically, the distance between the FITC label and the membrane surface was estimated to be in excess of 60 Å [40], and the distance between labeled cysteines 344, 364 (bracketing the phosphorylation residue Asp351) and the membrane surface was estimated to be ≈ 40 Å [41].

It is clear that the catalytic domain, and specifically the Asp351 residue undergoing phosphorylation, resides in the cytosolic region and is separated by a distance of ≈ 50 Å from the Ca^{2+} binding domain in the middle of the transmembrane region. In order to understand the mechanism of Ca^{2+} pumping it is essential to determine how the phosphorylation/dephosphorylation reaction is linked to the Ca^{2+} domain over such a large distance.

6. Modelling the calcium binding domain within clustered transmembrane helices

With the clear evidence that six residues distributed in four transmembrane helices are critical for Ca^{2+} linked functions in the Ca^{2+} ATPase we proposed a model in which these four helices cluster to form a tight channel-like structure within which Ca^{2+} binds [42]. Helices 4, 5, 6, and 8 in this cluster are positioned in such a way that each helix makes van der Waals contacts with its pair of neighbors (Fig. 4a). There are proline residues in helices 4, 6, and 8 which produce a slight "kink" in their helical structures. The helices are arranged so that the residues that are required for Ca^{2+} binding are oriented to the center of the channel produced by this cluster. It should be pointed out that helices 4, 5 and 8 (contributing only one residue each) can be rotated for optimal exposure of the Glu309, Glu771 and Glu908 side chains to the lumen of the channel. On the other hand, helix 6 contains three of the critical Ca^{2+} linked residues (Asn 796, Thr 799, Asp 800). In a strict helical structure only two of these residue side-chains ($CONH_2$ of Asp 796 and COOH of Asp800) would protrude from the same face of the helix, and participate directly in binding Ca^{2+}. In this orientation, however, the OH group of Thr799 would face the side of the channel, in a position closer to the adjacent helix. Therefore, the functional requirement for Thr799 must be explained either with a local deformation of helix 6 permitting exposure of the Thr799 OH to the center of the channel, or by a stabilizing function of this residue through interaction with another helix. A transversal section of the model (Fig. 4b) shows the protrusion of the critical side chains into the channel space. There is sufficient space in the channel to permit Ca^{2+} to move from one end to

Fig. 4. Model of the transmembrane Ca^{2+} binding site of Ca^{2+} ATPase. (a) Side view. Transmembrane helices 4, 5, 6 and 8 (see Fig 3) are clustered to form a Ca^{2+} binding channel. Because of the presence of prolines in the sequences, some of the helices are bent. The Ca^{2+} binding residues are arranged to face the central space at the middle of the helix cluster. A Ca^{2+} ion with van der Waals sphere is shown as a yellow ball in the center of the channel complexed with Ca^{2+} binding side chains. (b) Transversal view. In this view the transmembrane cluster of four helices is viewed from the cytosolic end. The helices starting from lower left and moving clockwise are 4, 5, 6, and 8. (c) Duplex Ca^{2+} binding site model for the Ca^{2+} ATPase. The four helices are shown again longitudinally, and were positioned to obtain the closest match to the duplex Ca^{2+} binding structure of thermolysin [43]. Four transmembrane helices of the SR Ca^{2+} ATPase contain the residues known to be critical for Ca^{2+} effects on activity. The six critical residues shown here were identified by site-specific mutagenesis studies. The model numbers shown here represent the position of the residues in their respective helices. These correspond to the sequence numbers: Glu9, Glu771; Glu 13, Glu309; Glu14, Glu908; Asn8, Asn796; Thr11, Thr799; Asp12, Asp800. Three Glu residues (9, 13 and 14) coordinate both Ca^{2+} ions. The upper Ca^{2+} is coordinated with Asp 12 while the lower Ca^{2+} coordinates with Asn 8. Helix 6 (which contains Asn 8, Thr 11, and Asp 12) is positioned with Asn8 and Asp12 coordinating the Ca^{2+} ions (as shown here), while the OH group of Thr 11 faces the side of the channel [44,45]. The centers of the two calcium ions are shown as two small circles – the lighter dotted lines represent the hydrogen bonds lattice.

the other; but the protruding side chains control the freedom of movement of Ca^{2+} ions in the middle of the channel.

A critical requirement of a Ca^{2+} binding model within the transmembrane region is that it should be consistent with a cooperative mechanism [11,46], which entails sequential binding of two Ca^{2+} per mol of ATPase from the cytosolic side of the membrane, and sequential displacement of the bound Ca^{2+} toward the lumenal side upon utilization of ATP (Fig. 5). Thus the model must ultimately provide for cooperative binding of two Ca^{2+} in single file within a transmembrane channel structure, and unidirectional movement of both ions across the membrane channel coupled with catalytic events in the cytosolic domain.

One clear example of a known protein structure exhibiting cooperative binding of two Ca^{2+} in close proximity to each other is thermolysin. In the crystal structure of thermolysin two Ca^{2+} that bound cooperatively reside in a duplex site with the Ca^{2+} ions only 3.8 Å apart [43]. The first site is heptacoordinate with pentagonal bipyramidal geometry while the second is hexacoordinate with octahedral geometry. A specific feature of this duplex binding site for Ca^{2+} in thermolysin is that three acidic side chains are shared by both Ca^{2+}.

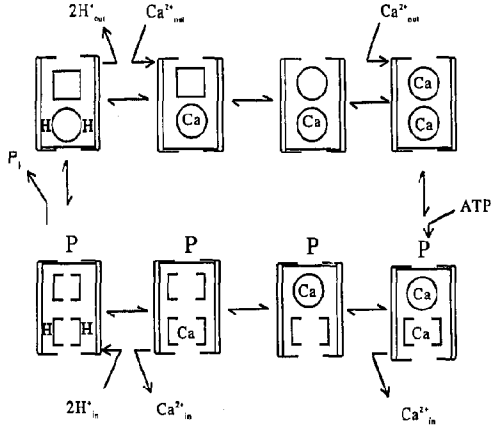

Fig. 5. Sequential positioning of two Ca^{2+} in single file within a channel in the ATPase membrane-bound region. Circles indicate a higher, and squares a relatively lower, affinity denoting the sequential development of cooperative binding. In the non-phosphorylated enzyme the outer Ca^{2+} is exposed to the cytosolic medium, and the inner Ca^{2+} is occluded. In the phosphorylated enzyme the inner Ca^{2+} has access to the lumenal medium, and the outer Ca^{2+} is transiently occluded. Ca^{2+} transport is accompanied by H^+ countertransport, related to exchange at the binding site.

Table 2
Ca^{2+} binding residues [a]

Thermolysin	Ca^{2+}ATPase
Asp 138	Glu 309 (helix 4)
Glu 177	Glu 771 (helix 5)
Asn 183 (carbonyl)	Asn 796 (helix 6)
Asp 185	Thr 799 (helix 6)
Glu 187 (carbonyl)	Asp 800 (helix 6)
Glu 190	Glu 908 (helix 8)

[a] List of residues involved in the duplex Ca^{2+} binding site in the thermolysin crystal structure [43], compared with residues involved in Ca^{2+} binding by the SR ATPase. Note the presence of four residues with acidic side chains in each structure. Simultaneous participation of Thr799 with Asn 796 and Asp800 in direct bonding with the ATPase Ca^{2+} is unlikely (see Figs. 5 and 7) unless helix 6 undergoes suitable conformational change (see text).

We have examined by molecular graphics [47] the structure of the Ca^{2+} ATPase transmembrane helices, and determined that there is a strong parallel between the thermolysin duplex Ca^{2+} binding ligands and the six residues identified with Ca^{2+} effects in the ATPase (Table 2). By adjusting the relative positions of the four helices within the membrane bilayer we can obtain a duplex binding site (Fig. 4c) similar to that of thermolysin. Note that the two sites have a vertical alignment analogous to that shown in Fig. 5. Furthermore, consider that contribution of residues by different helices renders the binding structure ideally suited to stabilization by Ca^{2+}, and destabilization of the resulting complex by forces imposed on the orientation of the helices (i.e. phosphoenzyme formation or thapsigargin binding). Recent studies on the effect of lumenal (inside) and medium (outside) pH on the stoichiometric ratios of H^+ and Ca^{2+} countertransport in proteoliposomes reconstituted with SR ATPase [48] indicate that the pK of the acidic residues participating in cation complexion changes to favor Ca^{2+} dissociation and H^+ binding as a consequence of ATP utilization. These

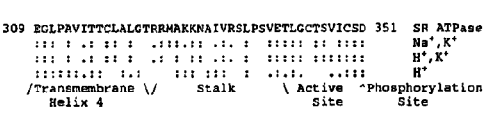

Fig. 6. Linker region homology. The amino acid sequences of four different ATP-linked cation pumps show little homology except in the region corresponding to residues 309 to 351. In the figure (:) denotes identity with the sequence of the ATPase; (.) denotes chemically similar residues; and a blank denotes a residue with no similarity to that of the SR ATPase. All four ATPases have an active site Asp corresponding to Asp351. All four also have Glu at a position corresponding to 309. In addition, the extensive homology and identity within this region indicate that this is a highly conserved region of all ATPases which likely serves a critical role in the protein function [49].

changes may be produced by slight displacement and/or rotation of the helices.

7. Linkage region between phosphorylation and cation binding domains

An interesting feature of the transmembrane channel involved in Ca^{2+} binding is that helix 4, which is the transmembrane helix containing Glu309, continues in the cytosolic space to Asp 351 which is the phosphorylation residue of the active site. This segment linking the phosphorylation site with the transmembrane region (corresponding to 309–351 in the SR Ca^{2+} ATPase (Fig. 3)) is highly conserved in other cation transport ATPases (Fig. 6). As there is little sequence homology between the Ca^{2+}-ATPase and the other cation ATPases except in this region, it seems likely that this homologous segment plays a key role in the linkage between ATP utilization and cation transport in all ATP-linked cation pumps. With respect to the Ca^{2+} ATPase, stabilization of the helical cluster by Ca^{2+} could be transmitted through this segment to the catalytic site, to produce catalytic activation by Ca^{2+} before ATP can be utilized. Conversely, local perturbations related to the phosphoryl transfer reaction at the catalytic site (e.g., inversion of phosphate oxygens) could be transmitted through this segment to the clustered transmembrane helices, producing vectorial destabilization of the Ca^{2+} complex. In fact, recent experiments on site-directed mutagenesis [50] have shown that the segment connecting phosphorylation and Ca^{2+} binding domains of the Ca^{2+} ATPase, is highly sensitive to single mutations resulting in inhibition of Ca^{2+} transport and catalytic turnover. Although the entire ATPase molecule should be considered to participate in the process of energy transduction, the peptide segment connecting the catalytic and Ca^{2+} binding domain is likely to function as a primary sensor of specific perturbations which may then be transmitted through alteration of the hydrogen bond lattice and repositioning of neighboring helices. It should be noted that long-range linkages originally proposed for hemoglobin by Wyman [51], appear to be a common mechanistic feature of diverse enzymes such as myosin [52], the λ repressor-operator complex [53] and the nitrogenase iron protein [54].

Acknowledgement

This work was partially supported by the National Institutes of Health (NHLB) and the American Heart Association.

References

[1] D.H. MacLennan, C.J. Brandl, B. Korczak and N.M. Green, Nature 316 (1985) 696.
[2] A.-M. Gunteski-Hamblin, J. Greeb and G.E. Shull, J. Biol. Chem. 263 (1988) 15032.
[3] J. Lytton and D.H. MacLennan, J. Biol. Chem. 263 (1988) 15024.
[4] S.E. Burk, J. Lytton, D.H. MacLennan and G.E. Shull, J. Biol. Chem. 264 (1989) 18561.
[5] A.M. Campbell, P.D. Kessler, Y. Sagara, G. Inesi and D.M. Fambrough, J. Biol. Chem. 266 (1991) 16050.
[6] W. Hasselbach and M. Makinose, Biochem. Z. 333 (1961) 518.
[7] S. Ebashi and F. Lippman, J. Cell Biol. 14 (1962) 389.
[8] G. Inesi, Ann. Rev. Physiol. 47 (1985) 573.
[9] G. Inesi, M. Kurzmack and D. Lewis, Meth. Enzymol. 157 (1988) 154.
[10] G. Inesi, M. Kurzmack and S. Verjovski-Almeida, Ann. NY Acad. Sci. 307 (1978) 224.
[11] G. Inesi, M. Kurzmack, C. Coan and D. Lewis, J. Biol. Chem. 255 (1980) 3025.

[12] C. Pickart and W.P. Jencks, J. Biol. Chem. 259 (1984) 1629.
[13] U. Rasmussen, S.B. Christensen and F. Sandberg, Acta Pharmaceut. Suec. 15 (1978) 133.
[14] O. Thastrup, Agents Actions 29 (1990) 8.
[15] Y. Sagara and G. Inesi, J. Biol. Chem. 266 (1991) 13503.
[16] J. Lytton, M. Westlin and M.R. Hanley, J. Biol. Chem. 266 (1991) 17067.
[17] Y. Kijima, E. Ogunbunmi and S. Fleischer, J. Biol. Chem. 266 (1991) 22912.
[18] Y. Sagara, F. Fernandez-Belda, L. De Meis and G. Inesi, J. Biol. Chem. 267 (1992) 12606.
[19] G. Inesi and Y. Sagara, Arch. Biochem. Biophys. 298 (1992) 313.
[20] Y. Sagara, J.B. Wade and G. Inesi, J. Biol. Chem. 267 (1992) 1286.
[21] G. Inesi and H. Asai, Arch. Biochem. Biophys. 126 (1968) 469.
[22] Y. Dupont, S. Harrison and W. Hasselbach, Nature 244 (1973) 554.
[23] D. Deamer and R. Baskin, J. Cell Biol. 42 (1969) 296.
[24] L.G. Herbette, P. DeFoor, S. Fleischer, P. Paolini, A. Scarpa and J.K. Blasie, Biochim. Biophys. Acta 817 (1985) 103.
[25] K.A. Taylor, L. Dux and A. Martonosi, J. Mol. Biol. 187 (1986) 417.
[26] D.L. Stokes and N.M. Green, Biophys. J. 57 (1990) 1.
[27] C. Toyoshima, H. Sasabe and D.L. Stokes, Nature 362 (1993) 469.
[28] G. Allen, B.J. Trinnaman and N.M. Green, Biochem. J. 187 (1980) 591.
[29] N.J. Karin, Z. Kaprielian and D.M. Fambrough, Mol. Cell. Biol. 9 (1989) 1978.
[30] D.J. Bigelow and G. Inesi, Biochim. Biophys. Acta 1113 (1992) 323.
[31] D.M. Clarke, T.W. Loo, G. Inesi and D.H. MacLennan, Nature 339 (1989) 476.
[32] C.C. Chadwick and E.W. Thomas, Biochim. Biophys. Acta 827 (1985) 419.
[33] C. Sumbilla, T. Cantilina, J.H. Collins, H. Malak, J.R. Lakowicz and G. Inesi, J. Biol. Chem. 266 (1991) 12682.
[34] C. Sumbilla, L. Lu, D.E. Lewis and G. Inesi, J. Biol. Chem. 268 (1993) 21185.
[35] C. Mitchinson, A. Wilderspin, B.J. Trinnaman and N.M. Green, FEBS Letters 146 (1982) 87.
[36] S. Wakabayashi, T. Imagawa and M. Shigekawa, J. Biochem. (Tokyo) 107 (1990) 563.
[37] S. Wakabayashi and M. Shigekawa, Biochemistry 29 (1990) 7309.
[38] J.E. Bishop, T.C. Squier, D.J. Bigelow and G. Inesi, Biochemistry 27 (1988) 5233.
[39] D.B. McIntosh, D.G. Woolley and M.C. Berman, J. Biol. Chem. 267 (1992) 5301.
[40] C. Gutiérrez-Merino, F.M. Munkonge, A.M. Mata, J.M. East, B.L. Levinson, R.M. Napier and A.G. Lee, Biochim. Biophys. Acta 897 (1987) 207.
[41] D.J. Bigelow and G. Inesi, Biochemistry 30 (1991) 2113.
[42] G. Inesi and M.E. Kirtley, J. Membr. Biol. 116 (1990) 1.
[43] M.A. Holmes and B.W. Matthews, J. Mol. Biol. 160(4) (1982) 623.
[44] G. Inesi, L. Lu and M.E. Kirtley, Cell Physiol. Biochem., in press.
[45] G. Inesi, Biophys. J., in press.
[46] G. Inesi, J. Biol. Chem. 262 (1987) 16338.
[47] M.E. Kirtley and G. Inesi, Proceedings from the 2nd IUBMB Conference on Membrane Biochemistry (1993).
[48] X. Yu, H. Luning and G. Inesi, J. Biol. Chem., accepted for publication.
[49] G. Inesi and M.E. Kirtley, J. Bioenerg. Biomembr. 24 (1992) 271.
[50] Z. Zhang, C. Sumbilla, D. Lewis and G. Inesi, FEBS Letters 335(2) (1993) 261.
[51] J. Wyman, Advan. Prot. Chem. 19 (1964) 223.
[52] J. Botts and M.F. Morales, Proc. Natl. Acad. Sci. USA 86 (1989) 2204.
[53] L.J. Beamer and C.O. Pabo, J. Mol. Biol. 227 (1992) 177.
[54] M.M. Georgiadis, H. Komiya, P. Chakrabarti, D. Woo, J.J. Kornuc and D.C. Rees, Science 257 (1992) 1653.